Prepared for submission to JHEP

Search for solar axions with CsI(Tl) crystal detectors

arXiv:1604.01825v3 [hep-ex] 23 May 2016

The KIMS Collaboration

Y.S. Yoon,[a] H.K. Park, [a,b,1] H. Bhang,[c] J.H. Choi,[c] S. Choi,[c] I.S. Hahn,[e] E.J. Jeon,[a] H.W. Joo,[c] W.G. Kang,[a] B.H. Kim,[c] G.B. Kim,[c] H.J. Kim,[f] K.W. Kim,[c] S.C. Kim,[c] S.K. Kim,[c] Y.D. Kim,[a,b,d] Y.H. Kim,[a,b,g] H.S. Lee,[a,b] J.H. Lee,[c] J.K. Lee,[c] D.S. Leonard,[a] J. Li,[a] S.S. Myung,[c] S.L. Olsen,[a] J.H. So,[a]

[a] *Center for Underground Physics, Institute for Basic Science (IBS), Daejon 34047, Korea*
[b] *Basic Science, IBS-UST School, Daejeon 34047, Korea*
[c] *Department of Physics and Astronomy, Seoul National University, Seoul 08826, Korea*
[d] *Department of Physics, Sejong University, Seoul 05006, Korea*
[e] *Department of Science Education, Ewha Womans University, Seoul 03760, Korea*
[f] *Department of Physics, Kyungpook National University, Daegu 41566, Korea*
[g] *Korea Research Institute of Standards and Science, Daejon 34113, Korea*
[h] *Department of Engineering Physics, Tsinghua University, Beijing 100084, China*
[i] *Institute of High Energy Physics (IHEP), Beijing 100049, China*

E-mail: hkpark@ibs.re.kr

Abstract: The results of a search for solar axions from the Korea Invisible Mass Search (KIMS) experiment at the Yangyang Underground Laboratory are presented. Low-energy electron-recoil events would be produced by conversion of solar axions into electrons via the axio-electric effect in CsI(Tl) crystals. Using data from an exposure of 34,596 kg · days, we set a 90 % confidence level upper limit on the axion-electron coupling, g_{ae}, of 1.39×10^{-11} for an axion mass less than 1 keV/c^2. This limit is lower than the indirect solar neutrino bound, and fully excludes QCD axions heavier than 0.48 eV/c^2 and 140.9 eV/c^2 for the DFSZ and KSVZ models respectively.

Keywords: axions, solar physics

[1] Corresponding author.

Contents

1 Introduction **1**

2 KIMS Experiment **2**

3 Data Analysis **3**

4 Summary **6**

1 Introduction

Despite its success, the Standard Model of particle physics still has many problems. One such problem, known as the strong CP problem [1], is that the CP-violating term in strong interaction implies that the neutron electric dipole moment has to be an order of 10^{10} larger than the experimental upper bound [2]. Peccei and Quinn [3] found out an elegant method to solve this problem by introducing a new global chiral symmetry $U(1)_{PQ}$ which is spontaneously broken at an energy scale f_a and which compensates the CP-violating term. This solution implies the existence of a new pseudoscalar particle called the axion (a) [4]. Since the original axion model assumed f_a to be at the electroweak energy scale, it was ruled out by laboratory experiments [5]. Currently the invisible axion models with the energy scale f_a as a free parameter, allowing up to the Plank mass scale of 10^{19} GeV, are not excluded by terrestrial experiments and astrophysics [6]. There are two popular models, the KSVZ (hadronic) [7] and DFSZ (non-hadronic) [8] models.

The strengths of axion-photon ($g_{a\gamma}$), axion-electron (g_{ae}) and axion-nucleon (g_{aN}) couplings are different for both models as described in ref. [9]. In particular, axion-electron coupling in the DFSZ model occurs at tree level while axion-electron coupling in the KSVZ model is strongly suppressed due to axion-electron coupling at loop level. Thus, in the DFSZ model, the processes related to axion-electron coupling [10–13] would prevail over the Primakoff process with axion-photon coupling as an axion production mechanism in stars and the sun: Compton scattering ($\gamma + e \rightarrow e + a$), axio-recombination ($e + A \rightarrow A^- + a$), axio-deexcitation ($A^* \rightarrow A + a$), axio-bremsstrahlung ($e + A \rightarrow e + A + a$), and electron-electron collision ($e + e \rightarrow e + e + a$), where A is an atom. The total axion flux on earth produced from the sun was recently estimated in ref. [14], which includes processes with axion-electron and axion-photon couplings, as shown in figure 1.

In this paper, we report on a solar axion search using the data sample from the KIMS experiment with CsI(Tl) crystal detectors. Since this estimation in ref. [14] does not have corrections for axions heavier than 1 keV/c^2, our search region for axions is below this value.

Axions would produce electron signals in the CsI(Tl) detector through the axio-electric effect, $a + A \rightarrow e^- + A^+$ where A is mainly either Cs or I in the detector. We searched

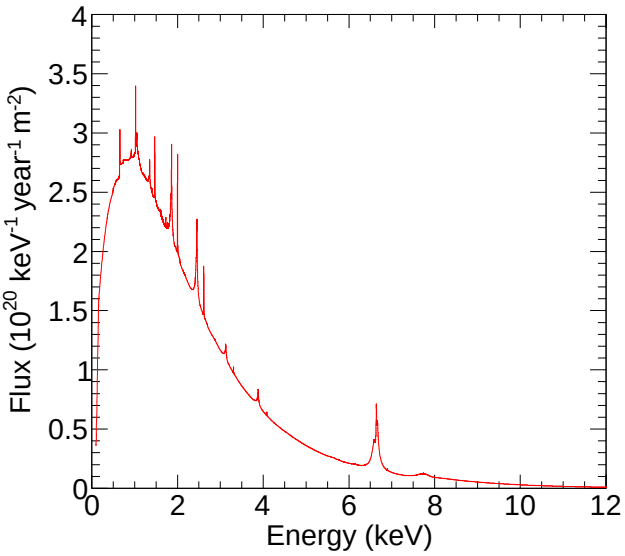

Figure 1. Flux of solar axions due to Compton scattering, axio-recombination, axio-deexcitation, axio-bremsstrahlung and electron-electron collisions on earth [14] with axion-electron coupling of $g_{ae} = 10^{-13}$.

for this process as a signal for solar axion detection. The cross section for the axio-electric effect [15] is given by

$$\sigma_{ae}(E_a) = \sigma_{pe}(E_a)\frac{g_{ae}^2}{\beta_a}\frac{3E_a^2}{16\pi\alpha m_e^2}(1-\frac{\beta_a^{\frac{2}{3}}}{3}), \tag{1.1}$$

where E_a is the axion energy, σ_{pe} is the photoelectric cross section for either Cs or I in ref. [16], g_{ae} is the axion-electron coupling, β_a is the axion velocity over the speed of light, α is the fine structure constant, and m_e is the electron mass. Figure 2 shows the cross sections for the axio-electric effect for Cs and I atoms with $g_{ae} = 1$.

2 KIMS Experiment

The KIMS experiment is designed to directly search for weakly interacting massive particles (WIMP) using CsI(Tl) crystal detectors. The experiment is housed in the Yangyang Underground Laboratory (Y2L) with an earth overburden of 700 m (2400 m water equivalent) and uses a 12 module array of low-background CsI(Tl) crystals with a total mass of 103.4 kg. Each detector module is composed of a CsI(Tl) crystal with dimension of 8 cm x 8 cm x 30 cm and with photomultiplier tubes (PMT) mounted at each end. The amplified signals from the PMTs on each crystal were recorded by a 400 MHz flash analog-to-digital converter for a duration of 32 μs with the trigger condition requiring at least two photoelectrons (PEs) in both PMTs on each crystal within a 2 μs window. The number of PEs are 5 to 6 per keV. The crystal array is completely surrounded from inside to outside by 10 cm of copper, 5 cm of polyethylene, 15 cm of lead, and a buffer consisting of liquid

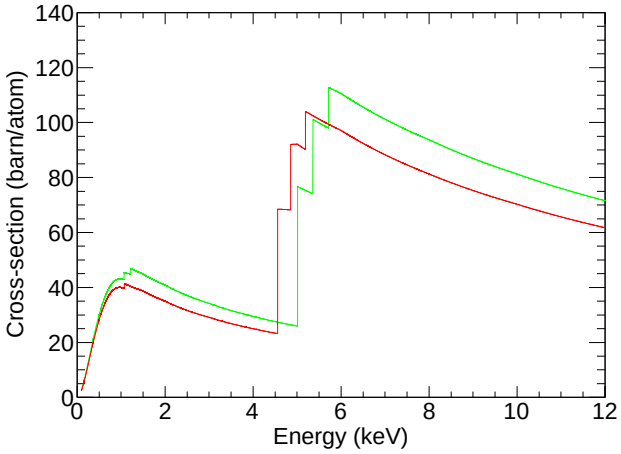

Figure 2. Axio-electric cross section calculated for Cs (green) and I (red) atom for axion mass of 0 keV/c^2 with $g_{ae} = 1$.

scintillator (LS) of 30-cm thickness. The LS buffer reduces external neutrons and gammas and is equipped with PMT's in order to reject cosmic-ray muon events. The experiment took stable data with 12 crystal modules in the period from September 2009 to December 2012. Details of the experiment can be found elsewhere [17–19].

3 Data Analysis

This analysis is based on one year data corresponding to an exposure of 34,596 kg·days. We applied event selection criteria that were developed for low-mass WIMPs search studies [19]. One of the main sources of background events is PMT noise. In order to reject these events, a set of event-selection criteria was developed by studying noise signals from a dummy detector module consisting of PMTs mounted on both ends of a transparent and empty acrylic box. The dummy detector was operated simultaneously with the CsI(Tl) detector array. These event-selection criteria were applied for the recorded events. In addition to these criteria, events induced by high-energy cosmic-ray muons were rejected by coincidence with the muon veto detector.

Events that passed the above selection criteria were divided into two independent event sets, single-detector (SD) and multiple-detector (MD) events. The MD events are defined as those for which multiple detectors each independently satisfied the trigger condition. Since an axion would give rise to an electron-like signal with a hit in only a single detector-module, only SD events were selected as axion candidate events. The SD events include surface α events (S_α) and electron recoil events (R_{e^-}) from Compton scattered γ rays and β decays in the crystal bulk [20]. The S_α events come from decays of radioactive isotopes which contaminate the surfaces of the crystals or the surrounding materials. Major internal backgrounds for β-decays in our CsI(Tl) crystals are ^{137}Cs (Q=1175.6 keV), ^{134}Cs (Q=2058.7 keV) and ^{87}Rb (Q=282 keV). The energy spectra from those radioisotopes are flat in our search region, 2 keV to 12 keV, as from Compton-scattered γ rays in the MD

events [20]. Therefore we expect that the MD energy spectrum is similar to the R_{e^-} spectrum in the SD sample. That is, the energy spectra for R_{e^-} events in the detector is expected to be a flat distribution in the axion search window. Pulse-shapes of photoelectron distributions in the time domain depend on the type of particle incident on the crystal. To discriminate R_{e^-} events from S_α events we employed the pulse-shape discrimination (PSD) method described in refs. [19, 21, 22]. In this method, the mean time (MT) for each event is calculated as follows:

$$MT = \int t f(t) dt / \int f(t) dt,$$

where $f(t)$ is the PE distribution. The quantity (LMT10) is obtained by taking base 10 logarithm of MT. The LMT10 distribution of each event type is well fitted by an asymmetric gaussian function defined as follows,

$$g(t) = \frac{A}{1/2(\sigma_L + \sigma_R)} e^{-\frac{1}{2}(\frac{t-\mu}{\sigma_L})^2}, \ t < \mu,$$
$$\frac{A}{1/2(\sigma_L + \sigma_R)} e^{-\frac{1}{2}(\frac{t-\mu}{\sigma_R})^2}, \ t \geq \mu,$$

where A is the amplitude, μ is the mean value and σ_L (σ_R) is the standard deviation of left (right) side. The parameters, μ, σ_L and σ_R, for the R_{e^-} events were first determined from the single-asymmetric-gaussian function fit to the MD sample data. In order to extract these fit parameters for S_α events, we applied fit to the data from a sample of a CsI crystal contaminated by ^{222}Rn progenies. With these parameters fixed, the contributions of R_{e^-} and S_α events in the SD data were determined by the fit and are shown in figure 3.

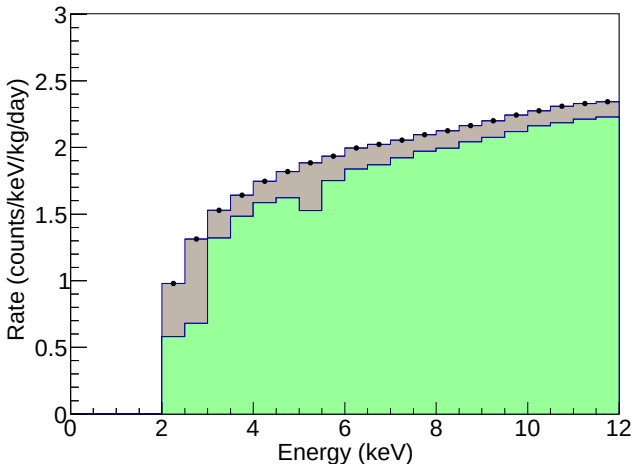

Figure 3. Contribution of electron recoil events (green) and surface alpha events (grey) to the observed single-detector energy spectrum (dots).

In our detector, the expected number of axion events is given by

$$R(E) = \int dE_a \frac{d\Phi_a}{dE_a} \epsilon(E) (\sigma_{ae}^{Cs}(E_a) N_{Cs} + \sigma_{ae}^{I}(E_a) N_I) T R_{det}(E, E_a)$$
$$\propto g_{ae}^4, \tag{3.1}$$

where $\frac{d\Phi_a}{dE_a}$ is the differential axion flux on the earth, $\epsilon(E)$ is the detection efficiency, $\sigma_{ae}^{Cs}(E_a)$ and $\sigma_{ae}^{I}(E_a)$ are the axio-electric cross section for Cs and I atoms, respectively, N_{Cs} and N_I are the number of Cs and I atoms, respectively, in our detector, T is the detector live time, and $R_{det}(E, E_a)$ is the resolution function of our detector.

The efficiency, $\epsilon(E)$, is estimated from the ratio of the number of MD events satisfying event selection cuts to the total number of MD events in each energy bin. The event selection efficiency is energy dependent and varies from 31.0% to 91.2%.

The resolution function, $R_{det}(E, E_a)$, is determined from a detector simulation. For each crystal, the photoelectron yield used in the simulation was estimated using data from the 59.4 keV γ generated from an ^{241}Am calibration source [19, 21].

To estimate the number of axion events, we used the energy spectrum for the R_e– events in the SD sample, which contains background events mainly from Compton scattered gamma rays and from β decays. The signal yield for axion event is extracted by maximizing a binned maximum likelihood function for the energy spectrum, which is given by

$$\mathcal{L} = \prod_{i=1}^{N_{bin}} e^{-(n_s P_s(E_i)+n_b P_b(E_i))} \frac{(n_s P_s(E_i) + n_b P_b(E_i))^{N_i}}{N_i!},$$

where N_{bin} is the number of bins, n_s and n_b are the expected number of signal and background events, respectively, N_i is the number of data events, and $P_s(E_i)$ and $P_b(E_i)$ are the probability density function (PDF) for signal and background in the energy bin E_i, respectively. The PDF for the energy spectra for the axion signal, $P_s(E)$, is constructed from the simulation by generating electron events with an energy distribution of $R(E)$. In order to model the background PDF below 12 keV, $P_b(E)$, we used the energy spectrum in the MD sample. This is possible because the spectrum contains only a flat Compton continuum, modified by the low-energy efficiency curve. Figure 4 shows the distributions for $P_s(E)$ and $P_b(E)$.

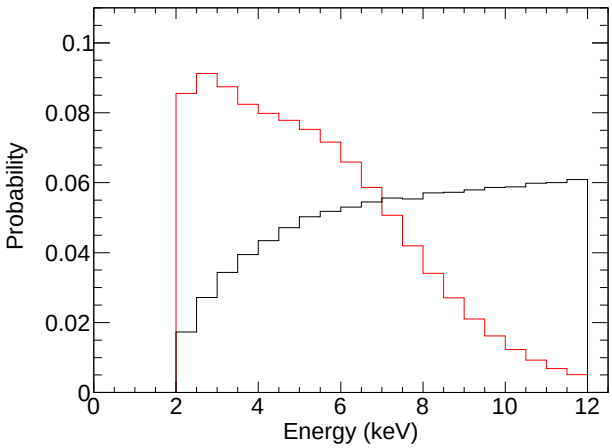

Figure 4. The PDF's for the axion (red) and background events (black).

The signal yields, n_s, for axion masses of 0 keV/c^2 to 1 keV/c^2 are found to be $0.077^{+36.59}_{-127.64}$ to $0.077^{+40.22}_{-132.12}$ events/year, consistent with no axion event. Figure 5 shows the energy distributions for R_{e^-} events in the SD sample, the background events (R_{e^-} events) in the MD sample estimated by the fit and axion signal events.

A 90 % confidence limit (C.L.) for the signal yield, n_s^{up}, is obtained from

$$\frac{\int_0^{n_s^{up}} \mathcal{L}(n_s)dn_s}{\int_0^{\infty} \mathcal{L}(n_s)dn_s} = 0.9. \tag{3.2}$$

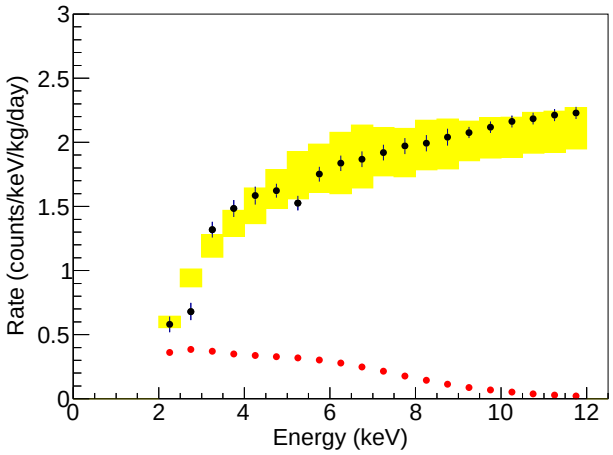

Figure 5. The energy distributions for the R_{e^-} events in the SD sample (black circle). The yellow shaded boxes are the background events estimated by the fit with the efficiency uncertainty. The red circles are the axion signals scaled up by a factor of million for better visibility.

The resulting values obtained for n_s^{up} are varied from 58.56 to 60.92 events with axion masses of 0 keV/c^2 to 1 keV/c^2. The upper limit on g_{ae} at the 90% C.L. is estimated with eq. 3.1, and is found to be $g_{ae} < 1.37 \times 10^{-11}$ and $g_{ae} < 1.39 \times 10^{-11}$ for axion mass of 0 keV/c^2 and 1 keV/c^2, respectively. From the upper limit on g_{ae}, we exclude a QCD axion heavier than 0.48 eV/c^2 in DFSZ model and 140.9 eV/c^2 in the KSVZ model.

4 Summary

A search for solar axions from 34,956 kg · days exposure with the KIMS CsI(Tl) detector array has been performed. In this search, we used the solar axion flux recently estimated with the DFSZ model assuming that axions produce electron signals in the CsI(Tl) detector through the axio-electric effect. The number of extracted axion events is consistent with no axion signal in this data sample. At the 90 % C.L., we obtain an upper limit of the axion-electron coupling, $g_{ae} < 1.39 \times 10^{-11}$ for axion mass of 0 keV to 1 keV and exclude QCD axions heavier than 0.48 eV/c^2 in the DFSZ model and 140.9 eV/c^2 in the KSVZ model. We exclude a region in the plane of axion mass and the axion-electron coupling at 90 % C.L. as shown in figure 6.

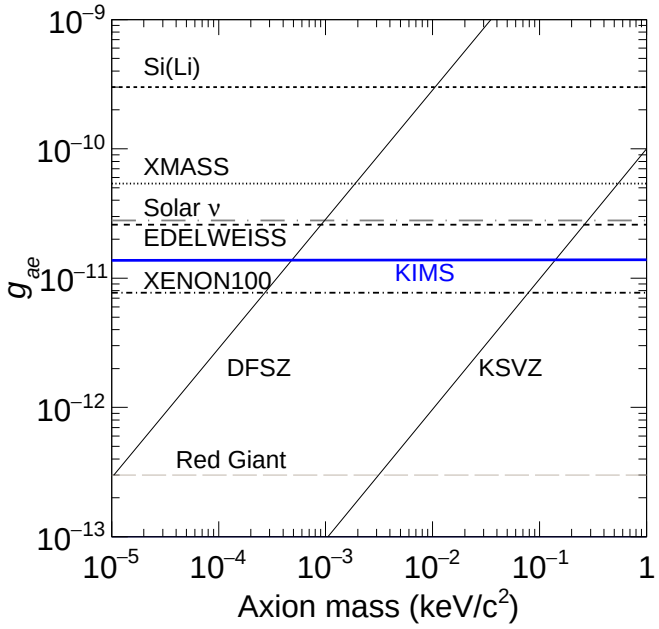

Figure 6. The blue line shows the 90 % C.L. on the axion-electron coupling (g_{ae}) for the KIMS. The dotted lines are limits by XMASS [23], EDELWEISS-II [24], XENON100 [25] and Si(Li) [26] experiments. The dash-dotted line shows indirect astrophysical bounds, solar neutrino [27] and red giants [28]. The gray lines are predictions by the KSVZ [7] and DFSZ [8] models.

Acknowledgments

We thank the Korea Midland Power Co. and Korea Hydro and Nuclear Power Co. for providing the underground laboratory space at Yangyang. We acknowledge support from the Institute for Basic Science (IBS) in Korea under the project code IBS-R016-D1, IBS-R016-D2, the WCU program (R32-10155), and the National Research Foundation of Korea (NRF-2011-0031280 and NRF-2011-35B-C00007).

References

[1] G. 't Hooft, Phys. Rev. Lett. **37**, 8 (1976); C.G. Callan, R.F. Dashen and D.J. Gross, Phys. Lett. **B 63**, 3432 (1976); R. Jackiw and C. Rebbi, Phys. Rev. Lett. **37**, 177 (1976).

[2] C.A. Baker *et al.*, Phys. Rev. Lett. **97**, 131801 (2006).

[3] R.D. Peccei and H.R. Quinn, Phys. Rev. Lett. **38**, 1440 (1977).

[4] S. Weinberg, Phys. Rev. Lett. **40**, 223 (1978); F. Wilczek, Phys. Rev. Lett. **40**, 279 (1978).

[5] T. W. Donnelly *et al.*, Phys. Rev. **D 18**, 1607 (1978); R. D. Peccei, ÒTheoretical Status Of Axions,Ó In *Wailea 1981, Proceedings, Neutrino Õ81; E.M. Riordan *et al.*, Phys. Rev. Lett. **59**, 755 (1987).

[6] K.A. Olive *et al.*(Particle Data Group), Chin. Phys. **C 38**, 090001 (2014).

[7] J.E. Kim, Phys. Rev. Lett. **43**, 103 (1979); M.A. Shifman, A.I. Vainstein, and V.I. Zakharov, Nucl. Phys. **B 166**, 493 (1980).

[8] A.R. Zhitnitskii, Yad. Fiz. 31, 497 (1980) [Sov. J. Nucl. Phys. 31, 260 (1980)]; M. Dine, F. Fischler, and M. Srednicki, Phys. Lett. **B 104**, 199 (1981).

[9] D.B. Kaplan, Nucl. Phys. **B 260**, 215 (1985); M. Srednicki, Nucl. Phys. **B 260**, 689 (1985).

[10] M. Fukugita, S. Watamura and M. Yoshimura, Phys. Rev. Lett. **48**, 1522 (1982); M. Fukugita, S. Watamura and M. Yoshimura, Phys. Rev. **D 26**, 1840 (1982).

[11] S. Dimopoulos *et al.*, Phys. Lett. **B 179**, 223 (1986); A. Derevianko *et al.*, Phys. Rev. **D 82**, 065006 (2010).

[12] L. M. Krauss, J. E. Moody and F. Wilczek, Phys. Lett. **B 144**, 391 (1984)

[13] G. G. Raffelt, Phys. Rev. **D 33**, 897 (1986).

[14] J. Redondo, JCAP **12**, 008 (2013).

[15] A. Derevianko *et al.*, Phys. Rev. **D 82**, 065006 (2010); M. Pospelov *et al.*, Phys. Rev. **D 78**, 115012 (2008).

[16] http://physics.nist.gov/PhysRefData/Xcom/html/xcom1.html

[17] H.S. Lee *et al.*(KIMS collaboration), Phys. Lett. **B 633**, 201 (2006).

[18] H.S. Lee *et al.*(KIMS collaboration), Phys. Rev. Lett. **99**, 091301 (2007).

[19] S.C. Kim *et al.*(KIMS collaboration), Phys. Rev. Lett. **108**, 181301(2012).

[20] T.Y. Kim *et al.*, Nucl. Instrum. Methods Phys. Res., Sect. A **500**, 337 (2003); H.S. Lee *et al.*, Nucl. Instrum. Methods Phys. Res., Sect. A **571**, 644 (2007).

[21] H. Park *et al.*, Nucl. Instrum. Methods Phys. Res., Sect. A **491**, 460 (2002).

[22] S.C. Kim *et al.*(KIMS collaboration), Astropart. Phys. **35**, 781 (2012).

[23] K. Abe *et al.*, Phys. Lett. **B 724**, 46 (2013).

[24] E. Armengaud *et al.*, JCAP **1311**, 067 (2013).

[25] E. Aprile *et al.*, Phys. Rev. **D 90**, 062009 (2014).

[26] A. Derbin *et al.*, JETP Lett. **95**, 339 (2012).

[27] P. Gondolo and G. G. Raffelt, Phys. Rev. **D 79**, 107301 (2009).

[28] N. Viaux *et al.*, Phys. Rev. Lett. **111**, 231301(2013).